AIP | Journal of Applied Physics

Strong heavy-to-light hole intersubband absorption in the valence band of carbon-doped GaAs/AlAs superlattices

M. I. Hossain, Z. Ikonic, J. Watson, J. Shao, P. Harrison et al.

Citation: J. Appl. Phys. **113**, 053103 (2013); doi: 10.1063/1.4790305
View online: http://dx.doi.org/10.1063/1.4790305
View Table of Contents: http://jap.aip.org/resource/1/JAPIAU/v113/i5
Published by the American Institute of Physics.

Strong heavy-to-light hole intersubband absorption in the valence band of carbon-doped GaAs/AlAs superlattices

M. I. Hossain,[1] Z. Ikonic,[2] J. Watson,[3,4] J. Shao,[3,4] P. Harrison,[2] M. J. Manfra,[1,3,4,5] and O. Malis[3,a)]

[1]*School of Electrical and Computer Engineering, Purdue University, West Lafayette, Indiana 47907, USA*
[2]*Institute of Microwaves and Photonics, School of Electronic and Electrical Engineering, University of Leeds, Leeds LS2 9JT, United Kingdom*
[3]*Department of Physics, Purdue University, West Lafayette, Indiana 47907, USA*
[4]*Birck Nanotechnology Center, West Lafayette, Indiana 47907, USA*
[5]*School of Materials Engineering, Purdue University, West Lafayette, Indiana 47907, USA*

(Received 1 January 2013; accepted 17 January 2013; published online 1 February 2013)

We report strong mid-infrared absorption of in-plane polarized light due to heavy-to-light hole intersubband transitions in the valence band of C-doped GaAs quantum wells with AlAs barriers. The transition energies are well reproduced by theoretical calculations including layer inter-diffusion. The inter-diffusion length was estimated to be 8 ± 2 Å, a value that is consistent with electron microscopy measurements. These results highlight the importance of modeling the nanoscale structure of the semiconductors for accurately reproducing intra-band transition energies of heavy carriers such as the holes. © *2013 American Institute of Physics*. [http://dx.doi.org/10.1063/1.4790305]

I. INTRODUCTION

Intersubband transitions within the conduction band of semiconductor quantum wells (QWs) have been widely explored in the past three decades, culminating with the development of high-performance devices such as the quantum-well infrared photo-detectors (QWIPs)[1] and the quantum cascade lasers (QCLs).[2] In contrast to their electronic counterparts, progress in understanding hole intersubband transitions and utilizing them for practical applications has been considerably slower. The hole intersubband transitions are particularly interesting because of their optical activity for both in-plane and out of plane light polarization, opening up the possibility of light emission or absorption perpendicular to the surface. For example, hole intersubband transitions between different kinds of hole states, such as between heavy and light hole states, are not subject to the same selection rules as electron intersubband transitions, i.e., the polarization of emitted or absorbed light is not restricted to the growth direction. Therefore, the hole intersubband transitions hold promise for novel optoelectronic devices such as mid-infrared vertical cavity surface emitting lasers (VCSELs). Moreover, recently there has also been renewed interest in hole-based photodetectors.[3,4]

Most of the research on hole intersubband transitions has been focused on Si/SiGe heterostructures,[5–8] due to interest in demonstrating a Si-based laser. Intersubband absorption, electroluminescence,[9–11] and photocurrent measurements have been reported in this material system. However, the Si/SiGe system suffers from challenges related to the growth of pseudo-morphic Si/SiGe heterostructures on various substrates and to the theoretical modeling of their strained band structure. To minimize these challenges, we are focusing on p-type GaAs/Al(Ga)As heterostructures. The arsenides represent an almost ideal model system for studying the mid-infrared optical properties of holes. This material system is virtually strain-free; the lattice mismatch between GaAs and AlAs is less than 0.2%. So, complex heterostructures can be grown with minimal strain build-up. Moreover, the valence bands of the AlGaAs alloys have their maxima at the respective Γ points throughout the compositional range, and therefore, the valence-band offset for GaAs/AlAs (0.5 eV) is comparable with the conduction-band offset of traditional QCL materials (InGaAs/InAlAs lattice-matched to InP). Therefore, the hole devices are expected to match the mid-infrared emission range which is most interesting for practical sensing applications. We have already demonstrated mid-infrared absorption[12–15] and electro-luminescence[15] from GaAs/AlGaAs heterostructures. Most relevant, our work highlighted the effect of layer inter-diffusion on the energy of hole intersubband transitions.[14] Our previous studies also revealed the challenges of understanding intra-valence band transitions between different types of hole states. In particular, the agreement between experimental results and theoretical calculations was only fair for heavy-to-light hole transitions. For this reason, this paper focuses on accurately measuring and modeling heavy-to-light hole intersubband transitions in dedicated C-doped GaAs/AlAs heterostructures. We found that inclusion of interdiffusion and many-body effects is critical to accurately reproduce the experimental heavy-to-light hole transition energies.

II. MATERIAL GROWTH AND CHARACTERIZATION

Solid source molecular beam epitaxy (MBE) was used to grow 3 GaAs/AlAs superlattices on GaAs (100) substrates. The structural details of the samples are given in Table I. To minimize interface roughness, the QW thicknesses were chosen to be exact multiples of the monolayer spacing, i.e., 15, 18, 21, for 42.5 Å, 50.9 Å, and 59.4 Å respectively. The barrier thicknesses were chosen to ensure localization of the first

a)Author to whom correspondence should be addressed. Electronic mail: omalis@purdue.edu.

TABLE I. Experimental data summary for the three different samples.

QW width (Å)	Barrier width (Å)	Periods	HH1-HH2 transition (*p*-pol) energy (meV)	HH1-LH2 transition (*p*-pol) energy (meV)	HH1-LH2 transition (*s*-pol) energy (meV)
42.5	73.6	50	163	252	254
50.9	62.3	50	128	218	216
59.4	62.3	50	104	171	175

excited light-hole states but thin enough to avoid extended defect generation during MBE growth. A solid carbon source was utilized for p-type doping of the QWs at a level of $1.2 \times 10^{12}\,\mathrm{cm}^{-2}$. The advantages of using C from a solid source over other sources for p-type doping are that it is compatible with high purity GaAs and has a lower diffusion constant. High-resolution X-ray diffraction measurements confirmed that the MBE-grown layer thicknesses are accurate to within 0.5 Å of the designed values. The samples were also examined with high resolution transmission electron microscopy (HR-TEM) and high-angle annular dark field scanning-transmission electron microscopy (HAADF-STEM) to characterize the interface quality (root mean square roughness, correlation length, and inter-diffusion length).

Mid-infrared absorption measurements were performed on samples polished in multi-pass waveguide geometry at 77 K using the temperature controlled cold finger of a helium-flow cryostat. The spectra were taken with a Thermo-Nicolet Fourier-transform infrared spectrometer equipped with a cooled HgCdTe detector in quick scan and the signal was averaged over 100 scans. A wire-grid polarizer was used to select the polarization of the incident radiation. *S*-polarization refers to an electric field parallel to the sample surface, while *p*-polarization corresponds to an electric field that forms an angle of 45° with the sample surface. To eliminate background absorption due to various optical components of the experimental setup, the *p*- and *s*-polarized spectra at 77 K were normalized to the corresponding spectra measured at room-temperature. Any room-temperature absorption is expected to be broad and weak and therefore was considered negligible.

III. BAND STRUCTURE AND ABSORPTION CALCULATIONS

The absorption calculations were done using the 6×6 k·p method, which accounts for full anisotropy and nonparabolicity of the valence subbands, as well as for the in-plane wave vector dependence of the optical transition matrix elements. Due to the rather high doping of the samples, the space charge effects (Hartree self-consistency) are accounted for, as well as the exchange correction in an approximate manner.[16,17] The depolarization effects in the optical absorption spectrum are also included.[7] The optical transition matrix elements for *s*-polarized light were calculated by allowing only for the in-plane component of the electric field. For *p*-polarization, the field had both in-plane and perpendicular components, with relative amplitudes depending on the incidence angle (e.g., equal to 45°), which is different from taking the average of squared matrix elements for the TE and TM waveguide polarizations. We note that for a particular transition, the ratio of absorption for the two polarizations depends sensitively on the angle of incidence, e.g., changing by a factor of 2-3 for ±10° variation of the angle.

IV. RESULTS AND DISCUSSION

The normalized *p*- and *s*-polarized absorption spectra at 77 K are shown in Figs. 1–3 for the 3 QW widths, 42.5 Å, 50.9 Å and 59.4 Å, respectively. Also, the experimental results for the peak positions are summarized in Table I. The low-energy peaks visible in each figure for *p*-polarized light only are due to transitions from the ground heavy-hole state (HH1) to the first excited heavy-hole state (HH2). The higher energy peaks dominating the *s*-polarized spectra but also visible in the *p*-polarized spectra are due to transitions between the HH1 state and the first excited light-hole state (LH2). It is immediately obvious that the energies of all experimental transitions are consistently higher than expected for QWs with abrupt interfaces, also shown in Figs. 1–3 (labeled id = 0 Å). We have previously observed this trend for heavy-to-heavy hole intersubband absorption in GaAs wells with digitally alloyed AlGaAs barriers[14] and attributed it to the valence-band distortion due to layer inter-diffusion at interfaces. To illustrate the effect of interdiffusion, each of the Figs. 1–3 also show the calculated *p*- and *s*-polarized absorption spectra for 2 values of the interdiffusion length (id), 6 Å and 10 Å, in addition to the calculations for no

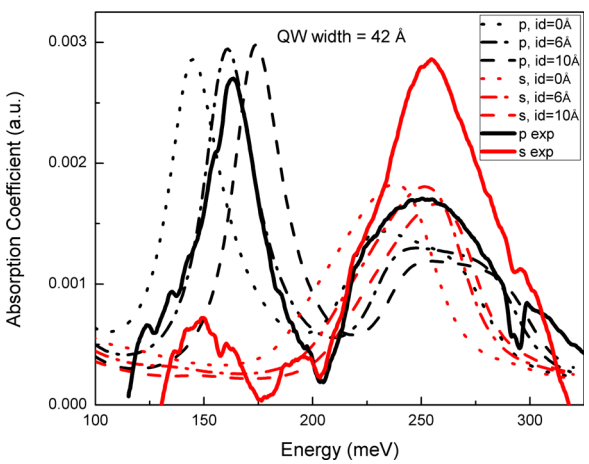

FIG. 1. Experimental and theoretical absorption spectra for the sample with 42 Å QWs at 77 K for *s*- and *p*-polarized light. The solid lines are experimental values while the discontinuous lines are theoretical simulations. The theoretical curves are displayed for three different interdiffusion lengths (id = 0, 6, and 10 Å).

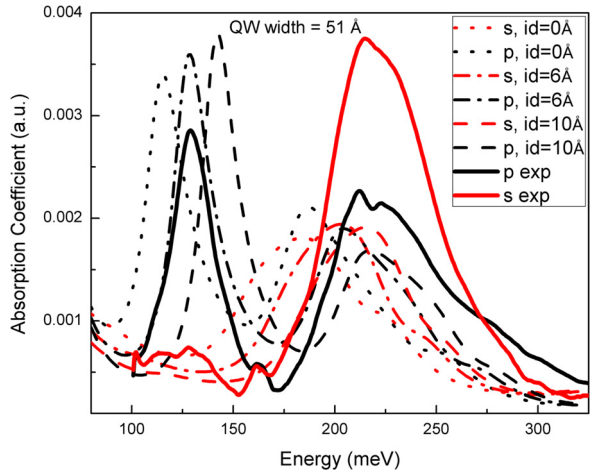

FIG. 2. Experimental and theoretical absorption spectra for the sample with 51 Å QWs at 77 K for *s*- and *p*-polarized light. The solid lines are experimental values while the discontinuous lines are theoretical simulations. The theoretical curves are displayed for three different interdiffusion lengths (id = 0, 6, and 10 Å).

interdiffusion (id = 0 Å). The details of the symmetric inter-diffusion model are given in Ref. 14. We do not expect that a slight asymmetry of the interfaces and/or dopant diffusion profile would play a major role on the absorption energy and linewidth. Besides the peak shifts, we also note that the HH1-LH2 transitions are stronger in both polarizations relative to the HH1-HH2 transitions in *p*-polarization than predicted theoretically. This effect can be explained at least in part by a deviation of the angle of incidence on the surface in the experiments from the targeted 45°.

To estimate the most likely value of the inter-diffusion length, the experimental energies for the HH1-HH2 transition (*p*-polarization) are compared with the theoretical values for several interdiffusion lengths in Fig. 4. Similarly, the experimental HH1-LH2 transition energies are compared with the results of the theoretical calculations as a function of inter-diffusion length in Figs. 5 and 6 for *s*- and *p*-polarized light, respectively. We found that no single inter-diffusion length fits

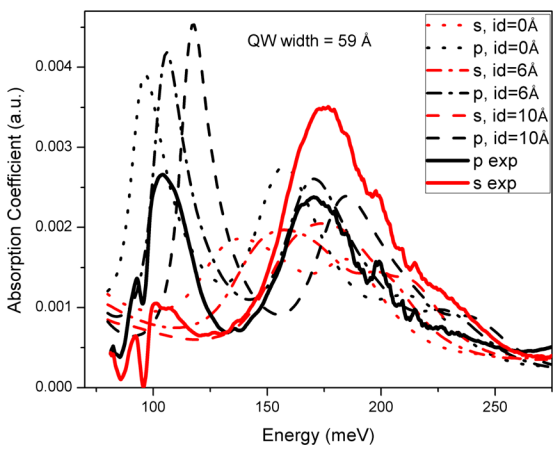

FIG. 3. Experimental and theoretical absorption spectra for the sample with 59 Å QWs at 77 K for *s*- and *p*-polarized light. The solid lines are experimental values while the discontinuous lines are theoretical simulations. The theoretical curves are displayed for three different interdiffusion lengths (id = 0, 6, and 10 Å).

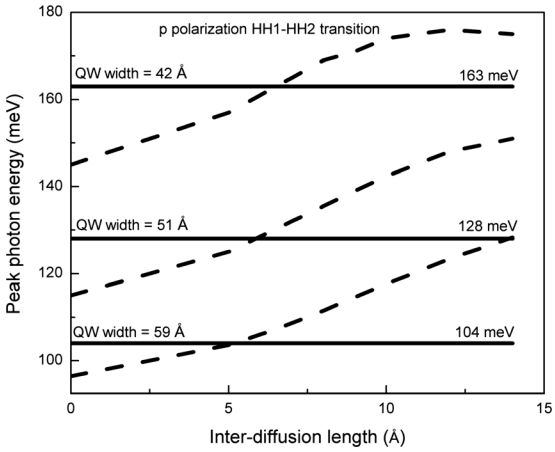

FIG. 4. Comparison of experimental HH1-HH2 hole transition energies measured with *p*-polarized light (horizontal lines) with results of theoretical calculations as a function of inter-diffusion length (dashed lines).

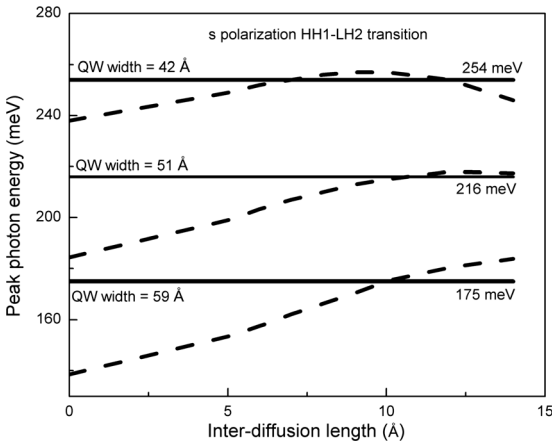

FIG. 5. Comparison of experimental HH1-LH2 hole transition energies measured with *s*-polarized light (horizontal lines) with results of theoretical calculations as a function of inter-diffusion length (dashed lines).

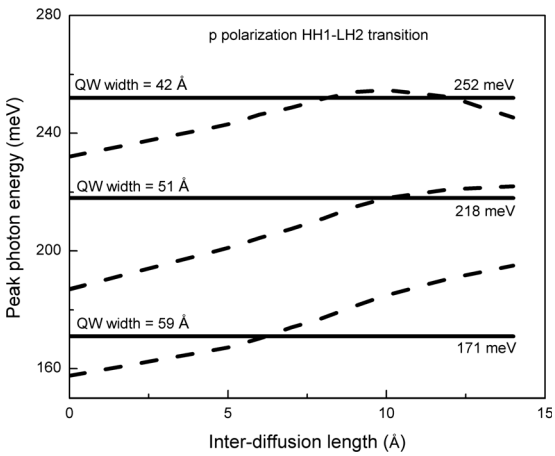

FIG. 6. Comparison of experimental HH1-LH2 hole transition energies measured with *p*-polarized light (horizontal lines) with results of theoretical calculations as a function of inter-diffusion length (dashed lines).

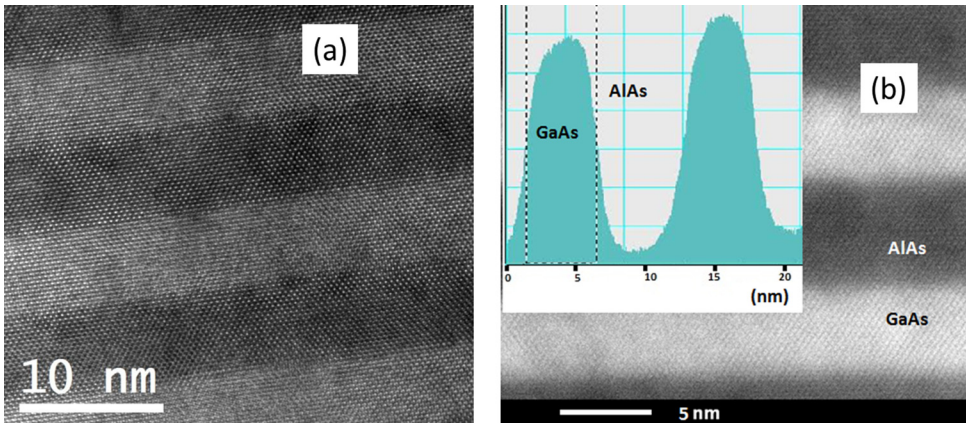

FIG. 7. (a) Bright field HR-TEM image with all beam condition of the sample with 51 Å quantum wells. (b) HAADF-STEM image of the same sample. The inset shows the atomic composition profile across several interfaces.

all samples and polarizations. It is noteworthy that the inter-diffusion length may vary from sample to sample due to slightly different growth parameters (growth temperature, time, etc.). However, we do expect the same inter-diffusion length to fit all peaks, for a particular sample. Therefore, we can only estimate the inter-diffusion length to be 8 Å ± 2 Å. This value is in agreement with estimates of the inter-diffusion length from HAADF-STEM measurements (Fig. 7(b)).

The uncertainty in the determination of the inter-diffusion length may be due to the small uncertainties in the experimental values of the QW widths and charge density, and/or our choice of normalization. We used the room temperature spectra for background subtraction, assuming the absorption is negligible at room temperature. Separate simulations (not included) showed that the effect of temperature on the HH1-LH2 transition is mainly seen for light polarized in the growth direction because it occurs only for finite in-plane wave-vector and increases with the magnitude of the k-vector. Hence, this absorption increases slightly with increasing temperature, as the hole distribution spreads in the k-plane. Since the light polarized perpendicular to the surface contributes only to the measured *p*-polarized absorption, this is why the *p*-polarized peak positions may depend more on temperature, particularly in the cases of the 51 Å and 59 Å QWs, where the HH3 state is near LH2, enhancing its non-parabolicity. In contrast, the *s*-polarized absorption energy is less affected by temperature, as it is dominated by contributions at small values of k-vector. Therefore, we consider the results from *s*-polarized spectra the most reliable.

In calculating the absorption spectra, the homogeneous part of broadening was assumed transition-dependent, but wave-vector independent, i.e., it was applied throughout the two subbands for a particular transition, and these values were determined so to fit the calculated line widths to the measured ones. These values (FWHM) were 26 meV (26 meV) for HH1-HH2 (HH1-LH2) transition in the 42.5 Å sample, 18 meV (30 meV) for HH1-HH2 (HH1-LH2) in the 50.9 Å sample, and 12 meV (28 meV) for HH1-HH2 (HH1-LH2) in the 59.4 Å sample. The homogeneous linewidths were also estimated from state lifetimes, by calculating the subband-averaged inter- and intra-subband hole scattering rates due to a number of scattering processes (acoustic phonon, polar LO phonon, deformation potential LO phonon, alloy disorder, ionized impurity, and interface roughness scattering).[14,18–20] The interface parameters for the grown samples were estimated from HR-TEM and HAADF-STEM measurements (Fig. 7) to amount to 4.1 Å for the root-mean square (rms) roughness and 17.5 Å for the correlation length. Such a calculation gives 25 meV, 17 meV, and 12 meV FWHM for the HH1-HH2 transition in the three samples, in surprisingly good agreement to the fitted values. However, the agreement is far less satisfactory (overestimate by a factor of ~3) for the HH1-LH2 transition, which indicates that the approximation of wave vector-independent scattering times (and hence also the homogeneous widths) should not be used for HH-LH transitions. However, a fully microscopic calculation was beyond the scope of this paper.

V. CONCLUSIONS

In conclusion, hole intersubband absorption in p-type GaAs QWs with AlAs barriers was measured in the mid-infrared range of the spectrum. The spectra exhibit narrow absorption peaks in *p*-polarized light due to heavy-to-heavy hole transitions and strong absorption in both *s*- and *p*-polarized light due to heavy-to-light hole transitions. Theoretical simulations considering layer inter-diffusion were found to better reproduce the experimental transition energies than previously reported. The estimated inter-diffusion length (8 ± 2 Å) is consistent with experimental estimates from scanning transmission electron microscopy measurements performed on the samples. The calculated linewidths for the heavy-to-heavy transitions are in agreement with the experimental measurements but overestimate the HH1-LH2 broadening. These results highlight the importance of modeling the nanoscale structure of the semiconductors for accurately reproducing experimental intra-band transition energies of heavy carriers such as the holes. Inter-diffusion is expected to be particularly important for design of complex optoelectronic devices, i.e., QWIPs and QCLs. These results may also prove valuable for other materials systems such as Si/SiGe and GaN/AlGaN.

ACKNOWLEDGMENTS

This work was supported by the NSF Award Nos. ECCS-1001431 and ECCS-0935899. We thank D. Zakharov of Purdue University for TEM characterization of the samples.

[1]H. C. Liu, Semicond. Semimetals **62**, 129 (2000).
[2]J. Faist, F. Capasso, D. L. Sivco, C. Sirtori, A. Hutchinson, and A. Y. Cho, Science **264**, 553 (1994).
[3]P. Rauter, G. Mussler, D. Grützmacher, and T. Fromherz, Appl. Phys. Lett. **98**, 21106 (2011).
[4]Y. F. Lao, P. K. D. D. P. Pitigala, A. G. U. Perera, H. C. Liu, M. Buchanan, Z. R. Wasilewski, K. K. Choi, and P. Wijewarnasuriya, Appl. Phys. Lett. **97**, 091104 (2010).
[5]K. Boujdaria, S. Ridene, S. Ben Radhia, O. Zitouni, and H. Bouchriha, J. Appl. Phys. **92**, 2586 (2002).
[6]Z. Ikonić, R. W. Kelsall, and P. Harrison, Phys. Rev. B **64**, 125308 (2001).
[7]T. Fromherz, E. Koppensteiner, M. Helm, G. Bauer, J. F. Nutzel, and G. Abstreiter, Phys. Rev. B **50**, 15073 (1994).
[8]S. K. Chun, D. S. Pan, and K. L. Wang, Phys. Rev. B **47**, 15638 (1993).
[9]L. Diehl, S. Mentese, E. Muller, D. Grutzmacher, H. Sigg, U. Gennser, I. Sagnes, Y. Campidelli, O. Kermarrec, D. Bensahel, and J. Faist, Appl. Phys. Lett. **81**, 4700 (2002).
[10]R. Bates, S. A. Lynch, D. J. Paul, Z. Ikonic, R. W. Kelsall, P. Harrison, S. L. Liew, D. J. Norris, A. G. Cullis, W. R. Tribe, and D. D. Arnone, Appl. Phys. Lett. **83**, 4092 (2003).
[11]I. Bormann, K. Brunner, S. Hackenbuchner, G. Zandler, G. Abstreiter, S. Schmult, and W. Wegscheider, Appl. Phys. Lett. **80**, 2260 (2002).
[12]O. Malis, L. N. Pfeiffer, K. W. West, A. M. Sergent, and C. Gmachl, Appl. Phys. Lett. **87**, 091116 (2005).
[13]R. Steed, M. Matthews, J. Plumridge, M. Frogley, C. Phillips, Z. Ikonic, P. Harrison, O. Malis, L. N. Pfeiffer, and K. W. West, Appl. Phys. Lett. **92**, 183104 (2008).
[14]Z. Ikonić, O. Malis, L. N. Pfeiffer, K. W. West, and P. Harrison, J. Appl. Phys. **107**, 113107 (2010).
[15]O. Malis, L. N. Pfeiffer, K. W. West, and A. M. Sergent, Appl. Phys. Lett. **88**, 081117 (2006).
[16]K. M. S. V. Bandara, D. D. Coon, O. Byungsung, Y. F. Lin, and M. H. Francombe, Appl. Phys. Lett. **53**, 1931 (1988).
[17]M. Tchernycheva, L. Nevou, L. Doyennette, F. H. Julien, E. Warde, F. Guillot, E. Monroy, E. Bellet-Amalric, T. Remmele, and M. Albrecht, Phys. Rev. B **73**, 125347 (2006).
[18]J. M. Hinckley and J. Singh, J. Appl. Phys. **76**, 4192 (1994).
[19]R. Scholz, J. Appl. Phys. **77**, 3219 (1995).
[20]M. Califano, N. Q. Vinh, P. J. Phillips, Z. Ikonić, R. W. Kelsall, P. Harrison, C. R. Pidgeon, B. N. Murdin, D. J. Paul, P. Townsend, J. Zhang, I. M. Ross, and A. G. Cullis, Phys. Rev. B **75**, 045338 (2007).